Jestr

Journal of Engineering Science and Technology Review 8 (2) (2015) 12-16
Special Issue on Synchronization and Control of Chaos: Theory, Methods and Applications

JOURNAL OF
Engineering Science and Technology Review

www.jestr.org

Research Article

Spectral Properties of Chaotic Signals Generated by the Bernoulli Map

Rafael A. da Costa[*, 1], Murilo B. Loiola[1] and Marcio Eisencraft[2]

[1]*Universidade Federal do ABC, Santo André, Brazil.*
[2]*Polytechnic School of the University of São Paulo, São Paulo, Brazil.*

Received 2 September 2014; Revised 4 October 2014; Accepted 25 October 2014

Abstract

In the last decades, the use of chaotic signals as broadband carriers has been considered in Telecommunications. Despite the relevance of the frequency domain analysis in this field, there are few studies that are concerned with spectral properties of chaotic signals. Bearing this in mind, this paper aims the characterization of the power spectral density (PSD) of chaotic orbits generated by Bernoulli maps. We obtain analytic expressions for autocorrelation sequence, PSD and essential bandwidth for chaotic orbits generated by this map as function of the family parameter and Lyapunov exponent. Moreover, we verify that analytical expressions match numerical results. We conclude that the power of the generated orbits is concentrated in low frequencies for all parameters values. Besides, it is possible to obtain chaotic narrowband signals.

Keywords: Chaotic signals, Bernoulli map, autocorrelation sequence, spectral analysis, piecewise linear maps.

1. Introduction

A chaotic signal is a deterministic and aperiodic signal that presents sensitivity on initial conditions [1]. This sensitivity means that the signals obtained with initial conditions near to each other can become very different when time passes [1]. There is a large number of research works involving applications of chaotic signal in several areas [2]. In Telecommunications, these researches were intensified after the seminal work by Pecora and Carroll [3]. Thereafter, the field of communication with chaotic carriers has received a great deal of attention, see e.g. [4,5,6] and the references therein.

As previously noted by [3], chaotic systems can be synchronized, allowing the development of many works regarding modulation schemes with chaotic signals as Chaos Shift Keying (CSK) and Differential Chaos Shift Keying (DCSK) [6,7]. They can transmit information by the coefficients of combination of sequences generated by chaotic signals. However, few studies analytically describe the spectral properties of chaotic signals, such as the Power Spectral Density (PSD). As every real world communication channel is bandlimited, to characterize and control the PSD of the generated chaotic signals is of paramount importance [6,8,9]. Therefore, the study of spectral characteristics is a relevant issue when it comes to using chaotic signals in practical communications.

The paper is divided into five sections. Section 2 defines the Bernoulli map $f_B(\cdot)$ and describes its main characteristics. In Section 3 the Autocorrelation Sequence (ACS) and PSD of the chaotic orbits generated by $f_B(\cdot)$ are deduced. In Section 4 the relationship between essential bandwidth and Lyapunov exponents is accessed. Finally, Section 5 presents our conclusion and possible applications of the results.

2. Bernoulli Map

In this paper, we consider the map

$$s(n+1) = f_B\left(s(n)\right) \tag{1}$$

with initial condition $s(0) \in [-1,\ 1]$ and $f_B : [-1,\ 1] \to [-1,\ 1]$ given by

$$f_B(s) = \begin{cases} \dfrac{2}{\alpha+1}s + \dfrac{1-\alpha}{\alpha+1}, & -1 \le s < \alpha \\ \dfrac{2}{1-\alpha}s - \dfrac{1+\alpha}{1-\alpha}, & \alpha \le s \le 1 \end{cases}, \tag{2}$$

which depends on the parameter $\alpha \in (-1,\ 1)$. Fig. 1(a) shows $f_B(s)$ for $\alpha = 0.8$ and in Fig. 1(b) the orbits $s(n)$ for $s(0) = -0.5$ and $s(0) = -0.500000001$ are depicted,

* E-mail address: r.costa@ufabc.edu.br

clearly showing the sensitivity on initial conditions characteristic of chaotic signals.

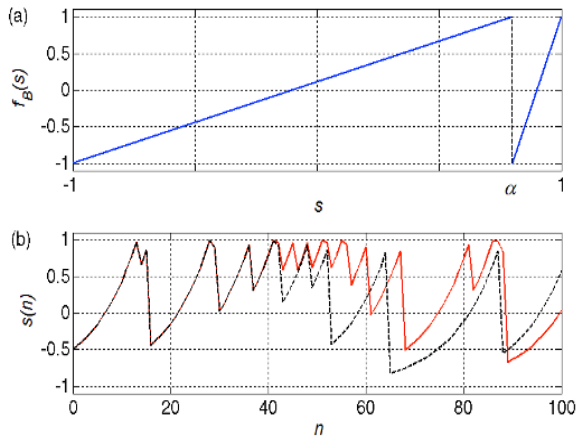

Fig. 1 (a) Bernoulli map $f_B(s)$ for α = 0.8; (b) orbits $s(n)$ for $s(0) = -0.5$ (continuous line) and $s(0) = -0.500000001$ (dashed line).

As shown in [10,11] the invariant density $p_*(s)$ of orbits of $f_B(\cdot)$ is uniform. In fact, $p_*(s) = 1/2$, for $-1 < s < 1$, for any α. This means that the orbit points are uniformly distributed on this interval. Consequently, these orbits are zero-mean and their average power is:

$$P = E[s^2(n)] = \frac{1}{3} \tag{3}$$

independently of α [10,11].

The Lyapunov exponent h_B of almost every orbit generated by $f_B(\cdot)$ is a function of α and can be calculated by [12].

$$\begin{aligned} h_B &= \int_{-1}^{1} \ln\left|f_B'(s(n,s_0))\right| p_*(s)ds \\ &= \int_{-1}^{\alpha} \frac{1}{2}\ln\left(\left|\frac{2}{1+\alpha}\right|\right)ds + \int_{\alpha}^{1} \frac{1}{2}\ln\left(\left|\frac{2}{1-\alpha}\right|\right)ds \\ &= \frac{1}{2}\left[(\alpha+1)\ln\left(\frac{2}{\alpha+1}\right) + (1-\alpha)\ln\left(\frac{2}{1-\alpha}\right)\right] \end{aligned} \tag{4}$$

where $f_B'(\cdot)$ is the derivative of $f_B(\cdot)$. As $h_B > 0$ for $\alpha \in (-1, 1)$, the aperiodic signals generated by $f_B(\cdot)$ are chaotic. The maximum value of h_B is ln2 occurring for α = 0, where the map $f_B(\cdot)$ generates chaotic signals with maximum exponential divergence.

In the following section, we derive the ACS and PSD of orbits generated by this map.

3. Autocorrelation Sequence and Power Spectral Density

Chaotic signals generated by a map can be treated as sample functions of an ergodic stochastic process [10]. For a fixed value of α, the signal generated by an initial condition $s(0)$ can be viewed as a sample function of the stochastic process defined by $f_B(\cdot)$. We can thus deduce the ACS and the PSD corresponding to $f_B(\cdot)$ as we usually proceed with ordinary stochastic processes. The following development is inspired by [9,13].

The ACS $R(k)$ of a signal $s(n)$ for an integer delay k is defined by

$$R(k) \equiv E[s(n)s(n+k)] \tag{5}$$

where the expected value $E[\cdot]$ is taken over all initial conditions that generate chaotic signals.

To simplify notation we define

$$s(n) \equiv x \quad \text{and} \quad s(n+k) \equiv y\,. \tag{6}$$

The joint density $p(x,y)$ is then given by

$$p(x,y) = p_*(x)\delta\left(y - f^k(x)\right) \tag{7}$$

where $p_*(x)$ is the invariant density of $f_B(\cdot)$ and δ is the Dirac unit impulse function [8]. Substituting (5) and (6) into (4) results in

$$\begin{aligned} R(k) &= E[xy] = \int_{-1}^{1}\int_{-1}^{1} xyp(x,y)dxdy \\ &= \int_{-1}^{1}\int_{-1}^{1} xyp_*(x)\delta\left(y - f_B^k(x)\right)dxdy \\ &= \frac{1}{2}\int_{-1}^{1} x f_B^k(x)dx. \end{aligned} \tag{8}$$

To evaluate (7), it is necessary to obtain $f_B^k(x)$ that means k-iterations of $f_B(\cdot)$. The map $f_B(\cdot)$ is composed of two linear segments. The image of each of these segments is the domain $U = [-1, 1]$. Fig.2 shows $f_B(x)$, $f_B^2(x)$, $f_B^3(x)$ and $f_B^k(x)$, for a generic k. We can deduce that when we iterate $f_B(\cdot)$ the number of its linear segments is multiplied by 2, i.e., $f^k(x)$ is formed by 2^k segments. The m^{th}-solution of the equation $f^k(x) = -1$ is represented by $a_k(m-1)$, $1 \le m \le 2^{k-1} - 1$ with $a_k\left(2^{k-1}\right) = 1$.

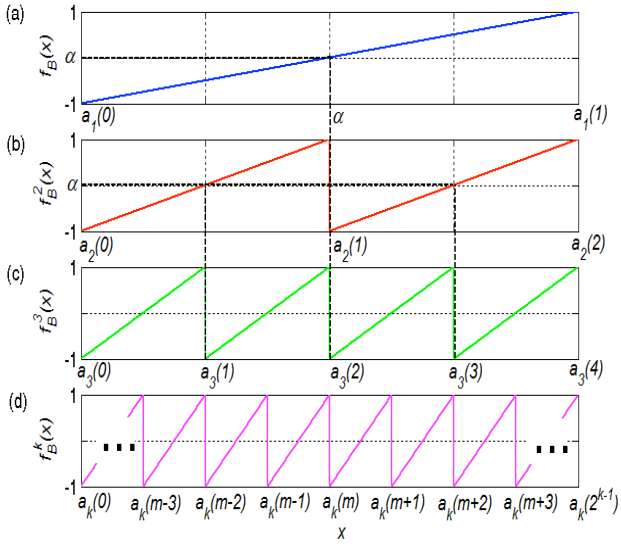

Fig. 2 (a) Bernoulli map $f_B(x)$ after (b) two iterations, (c) three iterations and (d) k-iterations.

This way, $f_B^k(x)$ in the interval $\left[a_k(m-1),\, a_k(m)\right]$ is given by

$$f_B^k(x)=\frac{2x-a_k(m)-a_k(m-1)}{a_k(m)-a_k(m-1)},\ a_k(m-1)\le x<a_k(m) \qquad (9)$$

Substituting (8) into (7), yields

$$R(k) \;=\frac{1}{2}\sum_{m=1}^{2^{k-1}}\int_{a_k(m-1)}^{a_k(m)} x\left(\frac{2x-a_k(m)-a_k(m-1)}{a_k(m)-a_k(m-1)}\right)dx \qquad (10)$$

By solving the integral in **Error! Reference source not found.**, we obtain

$$R(k) \;=\frac{1}{12}\sum_{m=1}^{2^{k-1}}\left[(a_k(m)-a_k(m-1))^2\right] \qquad (11)$$

The process of iterating the map one time, from $f_B^k(x)$ to $f_B^{k+1}(x)$, is illustrated in Fig. 3 where w is the root of $f_B^k(x)=\alpha$ and is given by

$$w \;=\frac{(a_k(m)-a_k(m-1))\alpha+(a_k(m)+a_k(m-1))}{2} \qquad (12)$$

From Fig. 3 the following relations can be inferred:

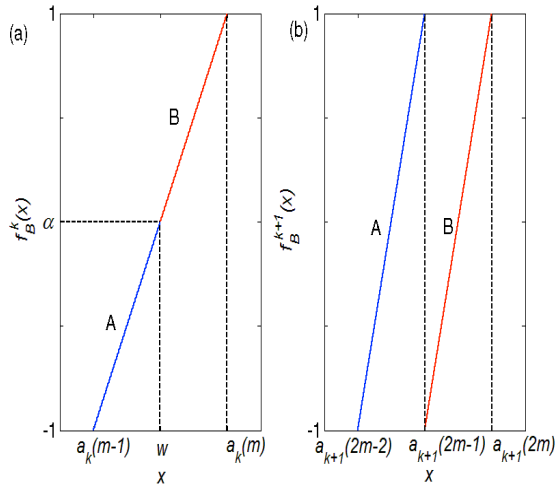

Fig. 3 (a) Generic stretch of $f_B^k(x)$ and (b) excerpt of this map after one iteration $f_B^{k+1}(x)$.

$$\begin{cases} a_{k+1}(2m-2) & = a_k(m-1) \\ a_{k+1}(2m-1) & = w \\ a_{k+1}(2m) & = a_k(m) \end{cases} \qquad (13)$$

Using (10) to evaluate $R(k+1)$ and substituting (12) and (11), $R(k+1)$ can be written as:

$$R(k+1) \;=\frac{1}{12}\frac{\left(1+\alpha^2\right)}{2}\sum_{m=1}^{2^{k-1}}\left[\left(a_k(m)-a_k(m-1)\right)^2\right] \qquad (14)$$

Comparing (13) with (10), it follows that

$$R(k+1) \;=\frac{(1+\alpha^2)}{2}R(k) \qquad (15)$$

Notice that $R(0)=E\left[s^2(n)\right]$ is the average power of $s(n)$ and is given by (2). Solving (14) with the initial condition $R(0)=\frac{1}{3}$, we obtain

$$R(k) \;=\frac{1}{3}\left(\frac{1+\alpha^2}{2}\right)^{|k|}. \qquad (16)$$

Figure 4 shows the ACS curves for some values of α. The dashed lines indicate the analytical result of (15) and the continuous lines the results of numerical simulation. Clearly, the numerical results agrees with (15). We observe that $R(k)$ decays monotonically faster to $|\alpha|\approx 0$ and slower for $|\alpha|\approx 1$. These results reveal that chaotic signals do not necessarily have impulsive ACS.

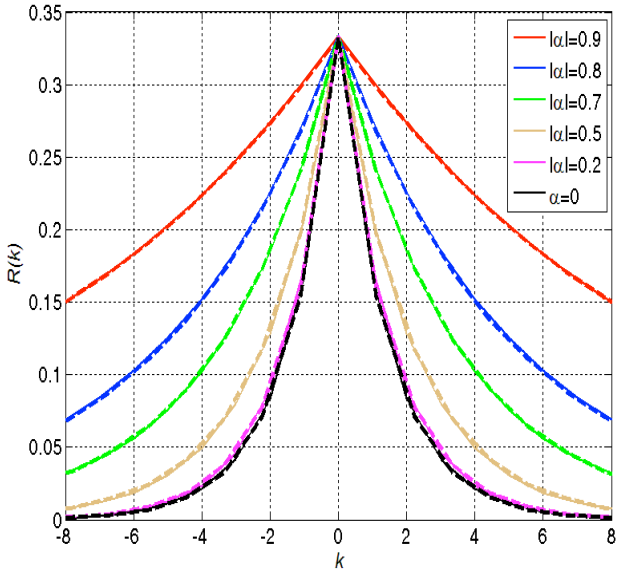

Fig. 4 Autocorrelation $R(k)$ for different values of α. The analytical result of (15) is shown in dashed lines and numerical simulations in continuous lines.

The PSD $P(\omega)$ is the discrete-time Fourier transform (DTFT) of $R(k)$, considering k as the time variable. Calculating the DTFT of (15), we obtain

$$P(\omega)=\sum_{k=-\infty}^{\infty}R(k)e^{-j\omega k}=\frac{1-\beta^2}{3(1+\beta^2-2\beta\cos(\omega))} \qquad (17)$$

with

$$\beta=\frac{1+\alpha^2}{2} \qquad (18)$$

Fig. 5 shows the PSD for some values of α. The dashed lines indicate the analytical result of (16) and the continuous lines the results of numerical simulation. Clearly, the numerical results agrees with (16). The value of α controls the way the power is distributed along the frequency axis. The

higher the absolute value of α, the smaller the frequency band where power is concentrated and vice versa.

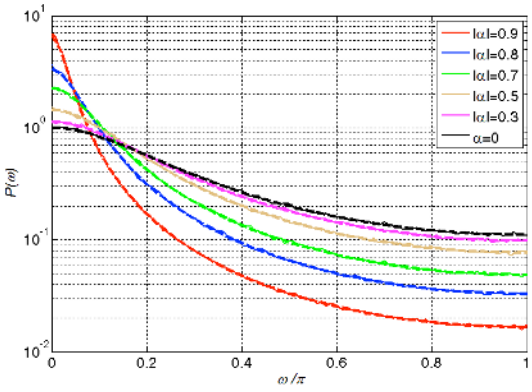

Fig. 5 Power spectral density $P(\omega)$ for different values of α. The analytical result of (16) is shown in dashed lines and numerical simulations in continuous lines.

4. Essential Bandwidth

The essential bandwidth B is defined as the length of the frequency interval where $q = 95\%$ of the signal power is concentrated [8]. To calculated B for a low-pass signal we must solve

$$\int_0^B P(\omega)d\omega = q\int_0^\pi P(\omega)d\omega \tag{18}$$

By using Parseval's Theorem [8] and (2)

$$\int_0^\pi P(\omega)d\omega = \frac{1}{3} \tag{19}$$

Substituting (16) and (18) in (17) and isolating B, we obtain

$$B = 2\arctan\left[\tan\left(\frac{q\pi}{2}\right)\left|\frac{\beta-1}{\beta+1}\right|\right] \tag{20}$$

with β given by (16).

Figure 6(a) shows $\frac{B}{\pi}$ as a function of $|\alpha|$ and Fig.6(b) shows $\frac{B}{\pi}$ as a function of the Lyapunov exponent h_B, given by (3). We observe an extremely narrowband process for $|\alpha| \approx 1$. As $h_B > 0$ for all values of α, we note that we can generate narrowband chaotic signals.

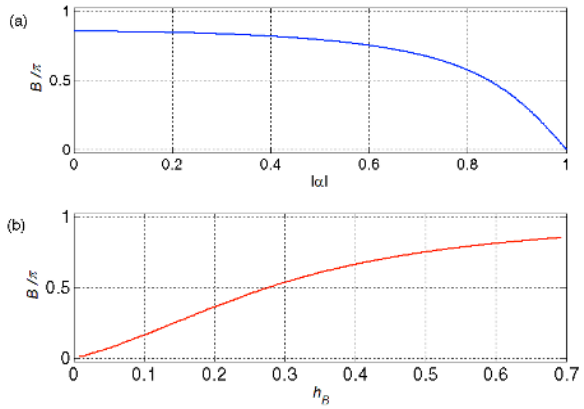

Fig. 6 Bandwidth $\frac{B}{\pi}$ as a function of (a) $|\alpha|$ and (b) Lyapunov exponent h_B.

5. Conclusion

In this paper, we have analytically deduced the ACS, PSD and essential bandwidth of the chaotic signals generated by the Bernoulli map.

Our main conclusion is that by adequately choosing the value of α, one can obtain chaotic signals with a desired bandwidth, with its power concentrated in the low frequencies range.

The analytical expressions presented in this paper confirm the possibility of easy generation of chaotic signals with a specific essential bandwidth. This means that the usual assumption about chaos implying broadband uncorrelated signals is not always true.

We have showed how α is related to the essential bandwidth B for the Bernoulli map. Hence, for a required B, from (19) the corresponding value of α can be determined and, consequently, the piecewise linear map that generates chaotic orbits with this particular B.

As future work, we intend to generalize the obtained results to more general piecewise linear maps consisting of an arbitrary number of segments.

6. Acknowledgments

The authors would like to thank CNPq-Brazil (grants 479901/2013-9 and 311575/2013-7), FAPESP (grant 2014/04864-2) and UFABC for their support on this research.

References

1. K.T. Alligood, T.D. Sauer, J.A. Yorke, Chaos-An ιntroduction to δynamical σystems, Springer, New York (1996).
2. S.H. Strogatz, Nonlinear δynamics and ψhaos: With αpplications to physics, biology, chemistry and engineering, Perseus Books Group, (2001).
3. L. Pecora and T. Carroll, Synchronization in chaotic systems, Physical Review Letters, vol. 64 (8), pp. 821-824 (1990).
4. F.C.M. Lau and C.K. Tse, Chaos-based digital communication systems, Springer, Berlin (2003).
5. M.P. Kennedy, R. Rovatti, and G. Setti, Chaotic electronics in telecommunications, CRC Press, Boca Raton (2000).
6. M. Eisencraft, R.R.F. Attux, and R. Suyama, (Eds.) Chaotic signals in digital communications, CRC Press, Inc. (2013).
7. G. Kolumbán., M.P. Kennedy, and L.O. Chua, The role of synchronization in digital communications using Chaos - Part II: Chaotic modulation and chaotic synchronization, IEEE Trans. Circuits Syst. I, vol. 45, pp. 1129 -1140 (1998).
8. B.P. Lathi, Modern digital and analog communication systems, Oxford University Press, New York (1998).

9. M. Eisencraft, D.M. Kato, and L.H.A. Monteiro, Spectral properties of chaotic signals generated by the skew tent map, Signal Processing, vol. 90(1), pp. 385-390 (2010).
10. A. Lasota and M. Mackey, Probabilistic properties of deterministic systems, Cambridge University Press, Cambridge (1985).
11. S. Tsekeridou, V. Solachidis, N. Nikolaidis, A. Nikolaidis, A. Tefas, and I. Pitas, Statistical analysis of a watermarking system based on Bernoulli chaotic sequences, Signal Processing, vol. 81, pp. 1273-1293 (2001).
12. C. Beck and F. Schögl, Thermodynamics of chaotic systems: An introduction. No. 4, Cambridge University Press (1995).
13. H. Sakai AND H. Tokumaru, Autocorrelations of a certain chaos, IEEE Transactions on Acoustics, Speech and Signal Processing, vol. 28(5), pp. 588-590 (1980).